Wind pressure coefficients for roof ventilation purposes

Gullbrekken, L., Uvsløkk, S., Kvande, T., Pettersson, K., & Time, B.

Citation for the published version (APA 6th)
Gullbrekken, L., Uvsløkk, S., Kvande, T., Pettersson, K., & Time, B. (2018). Wind pressure coefficients for roof ventilation purposes. Journal of Wind Engineering and Industrial Aerodynamics, 175, 144-152. doi:https://doi.org/10.1016/j.jweia.2018.01.026

Wind pressure coefficients for roof ventilation purposes

Lars Gullbrekken[1], Sivert Uvsløkk[2], Tore Kvande[1], Kaj Pettersson[3], Berit Time[2]

[1] Department of Civil and Environmental Engineering, Norwegian University of Science and Technology (NTNU), Trondheim, Norway

[2] Department of Materials and Structures, SINTEF Building and Infrastructure, SINTEF, Trondheim, Norway.

[3] Department of Architecture and Civil Engineering, Chalmers University of Technology, Gothenburg, Sweden

Abstract

Wind pressure coefficients (c_p) are important inputs for analytical calculations of wind load. The aim of this research is to investigate wind pressure coefficients on a test house located in Norway in order to pave the way for improved analysis of wind-driven roofing ventilation. The large-scale test measurements show that the wind pressure coefficient along the eaves of the house varies with different wind approach angles. Assuming wind-driven air flow through the air cavity beneath the roofing, an average $\overline{\Delta c_p}$ value of 0.7 is derived for practical engineering purposes. The results from the study are applicable for single or two-storey houses with pitched roofs at different roof angles.

1. Introduction

1.1 Background and scope

A load-bearing wooden roof is a proven and widely used type of construction in the Nordic countries. The various design principles for wooden roofs are thoroughly discussed by Edvardsen and Ramstad (2014). The basic principle is that the air cavity beneath the roofing must be ventilated to transport:

1. Moisture from the roof and thus prevent the growth of mould and moisture damage
2. Heat and thus prevent unwanted melting of snow and icing at the eaves and gutters

Roof ventilation guidelines for Norway are given by Bøhlerengen (2007, 2012) and are valid for roofs with a span less than 15 m and roof angle greater than 10° to 15°. A strong focus on CO_2-emissions from buildings most often favours wood-based materials and timber structures. Use of wood for the load-bearing system in roofs with increasingly longer spans and more complicated roof geometry is becoming more popular. In order to improve air cavity design guidelines for ventilated roofs it is necessary to increase the knowledge base for wind-driven ventilation of pitched roofs. The air change rate of the cavity is given by driving forces from wind and temperature differences (natural convection) together with pressure losses in the system. To calculate the wind-driven ventilation of such a roof it is necessary to calculate the difference in wind pressure coefficient, c_p, at the inlet and the exit of the air cavity. This difference is hereafter defined as Δc_p.

This work is based on measurements performed by Uvsløkk in 1985 and the work was previously partly published in Uvsløkk (1996). However, the scope of Uvsløkk (1996) was limited to examine the wind pressure gradients in the air cavity behind a ventilated cladding.

The aim of this research has been to investigate c_p at the wall surface of a test house located in Norway. In section 1.2-1.6 the theoretical framework for the wind pressure coefficient (c_p) and relevant past research on it are presented. In section 2 the experimental design and implementation

used in this paper is presented. In sections 3 and 4 the results and a discussion of the implications are given, respectively. Section 5 consists of final thoughts and conclusions. The c_p at the air cavity openings of the roof, together with the wind velocity and wind approach angle, defines the driving forces of wind-driven air cavity ventilation. Therefore, knowledge about such parameters is necessary when calculating wind-driven air cavity ventilation of pitched roofs.

1.2 Wind pressure coefficient

The wind pressure coefficient at a point is defined as wind pressure at the point divided by the dynamic pressure in free wind at a reference height above ground, normally 10m (NS-EN 1991-1-4:2005):

$$c_{px} = \frac{P_x - P_0}{P_d} \quad (1)$$

$$P_d = \frac{\rho \cdot U^2}{2} \quad (2)$$

c_{px} is the wind pressure coefficient of a point (-), P_x is the static pressure at point x on the building facade (Pa), P_0 is the static reference pressure (Pa)(at 10m height), P_d is the dynamic pressure (Pa), ρ is the air density (kg/m³) and U is the wind speed at 10m (m/s).

Δc_p is defined by equation (3) and (4), where c_{px1} and c_{px2} are wind pressure coefficients at the positions shown in Figure 1.

$$\Delta c_{px} = c_{px1} - c_{px2} \quad (3)$$

$$\Delta c_p(\theta) = c_p(\theta) - c_p(180-\theta) \quad (4)$$

Where θ is the wind approach angle (horizontal)

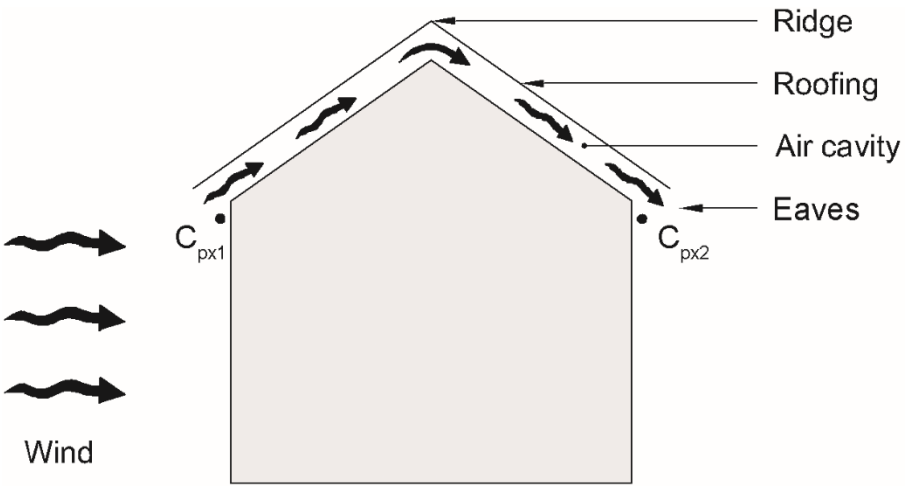

Fig. 1 Cross-section of a house showing the location of the two pressure points for calculation of Δc_{px}.

There are three methods to estimate c_p: full-scale test, a model test in a laboratory wind tunnel and by parametric equations derived from experiments. For a specific building, a fully accurate determination of c_p can only be done using a full-scale test (Bartko et al. 2016, Uvsløkk 1996) or a model test (Tominaga et al. 2015, Quan et al. 2011) of the specific building. Full-scale

measurements are costly, difficult and require expertise, and consequently are only performed on complex and high rise buildings in order to develop parametric equations.

1.3 Full-scale tests

Wells and Hoxey (1980) performed full-scale wind coefficient measurements mainly on roofs of five different glasshouses situated in the UK. The measurements were done with the aim to increase knowledge about design values of wind coefficients of such buildings. Richardson and Surry (1991) performed comparisons of full-scale and model-scale measurements, focusing on mean wind pressure coefficients of four low-rise buildings. The mean pressure coefficients presented for four buildings suggested that a wind tunnel does not accurately model the separation of the flow on the windward roof. Full-scale measurements of side wall pressure coefficients reported for three buildings indicated a Δc_p across the air cavity of the roof of 0.6-1.0.

Wind pressure coefficients on a specific part of a building were calculated by Caracoglia and Jones (2009). The facade-measurements were performed close to a corner of the building which had a complex geometry. Wind-induced response on low-rise buildings by use of load cells in the foundation system of the building and in the wall/roof joint was investigated by Zisis and Stathopoulos (2012). For the mean wind pressure coefficient, the full-scale measurements showed excellent agreement with the model (wind tunnel) results given a suburban terrain. Given an open and light suburban terrain and a wind angle of 60 degrees to the long wall of the test model, Figure 6 in Zisis and Stathopoulus (2012) indicates a Δc_p across the air cavity of 0.5. Further, the results interpret a larger Δc_p in a more suburban terrain however it should be noted that the measurements only included one wind direction.

1.4 Model test

Kanda and Maruta (1993) performed model measurements of wind coefficients on a long low-rise building with a gable roof. On the windward wall they measured a wind pressure coefficient between 0.5 and 0.8 depending on the roof pitch. A thorough literature review of wind pressure measurements, using both field studies and model studies, was conducted by Uematsu and Isyumov (1999). They found a number of research efforts trying to determine wind loads on low-rise buildings. However, the authors still pinpointed the need for more measurement data to cover different variables.

Blom (1990) also performed model measurements using an identical downscaled model of the test house used in this study. However, the measurements were simplified and included, for example, only one wind approach angle.

Yang et al. (2008) performed model testing in a wind tunnel and compared the results to calculations, however, the measurements were only performed on a limited range of wind approach angles.

Tominaga et al. (2015) conducted wind tunnel experiments to examine air flow around building models and the results were used to validate a Computational Fluid Dynamics (CFD)-model. The model dimension were L x W = 6.6 X 6.6m and height from ground to eaves of 6m. Three different roof angles of 16.7, 26.6 and 36.9° with no roof overhang were tested. The model was oriented perpendicular to the flow. Although taking measurements of the driving forces for ventilation the air cavity beneath the roofing was not in the scope of the work, the study indicates a Δc_p across the air cavity of 1.1-1.4 for all the investigated roof angles (Figure 2).

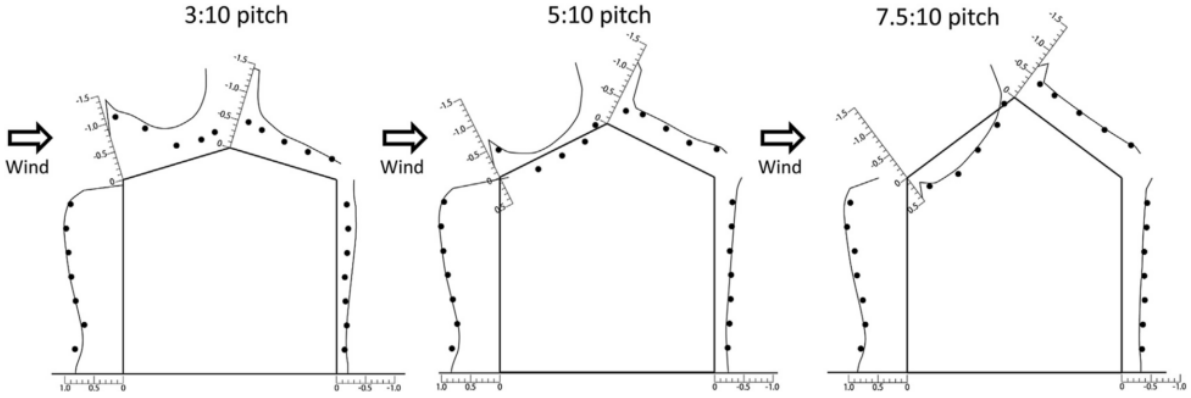

Fig. 2 Black dots represent measurements of c_p for a model house. Three different roof angles were studied. Figure from Tominaga et al. (2015).

The c_p of the pitched roof is significantly influenced by the roof geometry of low-rise buildings (Xu and Reardon 1998, Blom 1990). Xu and Reardon (1998) performed wind tunnel measurements on a building model with 15°, 20° and 30° roof pitches and large overhangs. They found that a roof angle of 30° experienced the highest negative c_p at the roof corner compared to the 15°- and 20°-roof angle. Blom (1990) performed model measurements using an identical model of the test house used in the current study. He also concluded that the roof angle influences the distribution of c_p of a pitched roof.

Furthermore, Ahmad and Kumar (2002) studied the mean pressure coefficients on elevated and single-storey houses. By assuming the situation given in Figure 1, the results from their study indicate a Δc_p across the air cavity of 0.6-1.3 depending on the height of the building.

1.5 Parametric equations

Muehleisen and Patrizi (2013) developed simplified parametric equations that more accurately describe the performance of isolated buildings. The study only included a flat roof configuration.

A thorough overview of pressure coefficient data and to what extent the data is currently implemented in building energy simulation and airflow network programs was performed by Cóstola et al., (2009). The following primary sources of data were mapped: full scale measurements, reduced scale measurements in wind tunnels and CFD (computational fluid dynamics) simulations. In addition, secondary sources such as databases and analytical models were studied. Cóstola et al., (2009) found that a wide range of parameters influence the pressure coefficients on building facades. A high uncertainty was also associated with pressure coefficients of buildings sheltered by neighbouring buildings.

The Eurocode 1 standard (NS-EN 1991-1-4:2005) gives instructions for calculation of wind strains on building facades.

1.6 Knowledge gap

Several full-scale and model scale studies of c_p on facades and roofs have been conducted. However, to the authors' knowledge, there are few studies of specific measurements of the c_p at the inlet and the outlet of the air cavity beneath the roofing of a pitched roof, defined by the authors as Δc_p. Analysis of the measurements by Tominaga et al. (2015), Zisis and Stathopoulos (2012) and Richardson and Surry (1991) indicates a Δc_p of 0.5 to 1.4, which represents a rather large span. This study is undertaken in order to more precisely derive a Δc_p applicable for an engineering evaluation of air cavity design.

2. Method

2.1 Test set-up

A test house located at an open field test station in Tyholt, Trondheim, (63.4222N, 10.4302E) 110m above sea level was equipped with instrumentation for wind pressure measurements (see Figure 3). The building was 8m long, 5m wide and the height to the top of the roof was 6m. The roof angle was 38° and the attic space was ventilated through an opening along the eaves as shown in Figure 3 and 4. The roof (ceiling), walls and floor were insulated. By use of an electric motor, the test house could be rotated making it possible to carry out wind pressure measurements for all parts of the walls at any wind approach angle. The ground at the test site was even and open with no trees or buildings within a distance of about 150m in a sector from south-southeast to southwest which was the dominating wind direction during the measurement periods. Wind speed was measured by a Lambrecht anemometer positioned 6m above ground level in a mast positioned 40m away in a west northwest direction from the test house, as Figure 3 shows. Wind speed was also recorded by an identical anemometer located in the centre of the house, 4m above the ridge and 10m above ground level. This was to investigate the influence of the test house on the flow pattern of the wind.

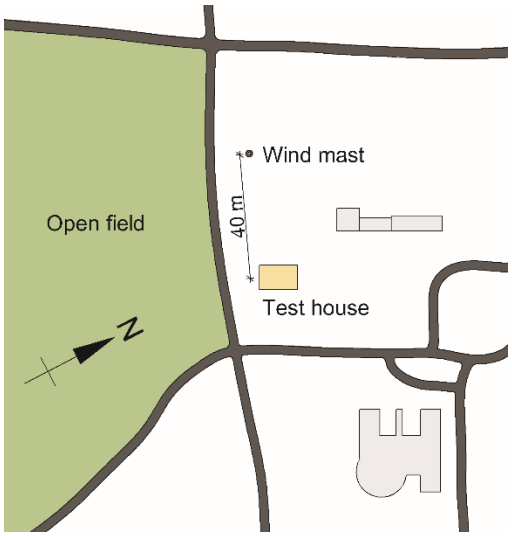

Fig. 3 Position of test house and wind mast at the field test station.

Four groups of pressure measurement points were located on the long wall (see Figure 4). In addition, two groups of pressure points were located on the short wall of the house. Eight pressure points in each group were distributed along a vertical line: four located in the air gap between the cladding and the wind barrier, and four on the exterior surface of the cladding. The wind pressure was measured using plastic tubes which were coupled to pressure transducers inside the test house. All the tubes were 10m long and had an interior diameter of 4mm. At each exterior measuring point a plastic tube was coupled to a brass tube with the opening at the surface of the cladding. The brass tubes were 50mm long and had an interior diameter of 3mm. The 20 pressure transducers were Furnes Transducer FCO 40 (0-1000Pa) micro manometers. Of the 20 transducers, 16 were attached to the different pressure tubes. The remaining four were coupled to fixed measuring positions as follows: dynamic wind pressure at 10m above ground level, air pressure inside the house, wind pressure in the attic and wind pressure in a fixed position on the long wall. The pressure transducers reported the pressure difference between the wind pressure at the measuring point and the reference static pressure. Reference static pressure was measured in a mast 10m above ground, 4m above the ridge of the house and in the centre of the house (see Figure 4). This was done by attaching all the pressure transducers to a plastic tube which ended at the surface of a vertical aluminium plate designed as a wind vane. Dynamic pressure and wind approach angle were also registered in this mast based on the principle presented in Hoxey and Wells (1974, 1977).

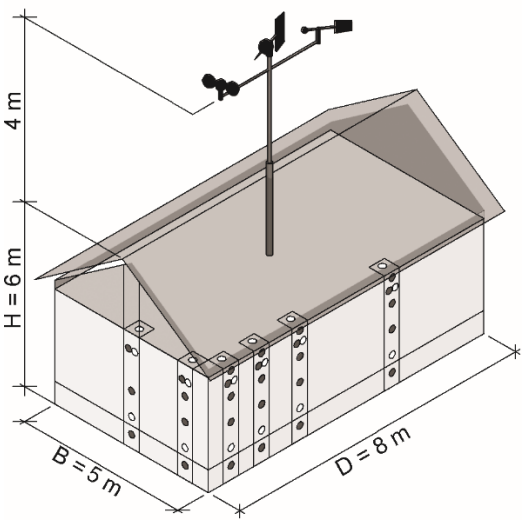

Fig. 4 The rotatable test house located in Tyholt in Trondheim used for wind pressure measurements.

In advance of each measuring period, the tubes were cleaned by use of pressurised air. The pressure transducers were zeroed before and after each measurement series. Twenty values from each pressure transducer were recorded during the measurement period of ten seconds. Then, the test house was rotated to achieve a slightly different wind approach angle and the procedure was repeated. During stable wind all the measurements could be conducted within a couple of hours. Usually the measurements were repeated on another day in 15 to 25 different wind approach angles for all measuring positions.

Three construction variants have been investigated; two of these are shown in this paper in Figure 5. The only difference between the construction variants is the horizontal wooden board. The main purpose of the board is to reduce rain and snow drifting into the attic. The horizontal part of the eaves was 100mm. The third construction variant is not included because it was identical to variant 1 except for the design of the air cavity behind the cladding. In addition, the measurement data for this variant was limited.

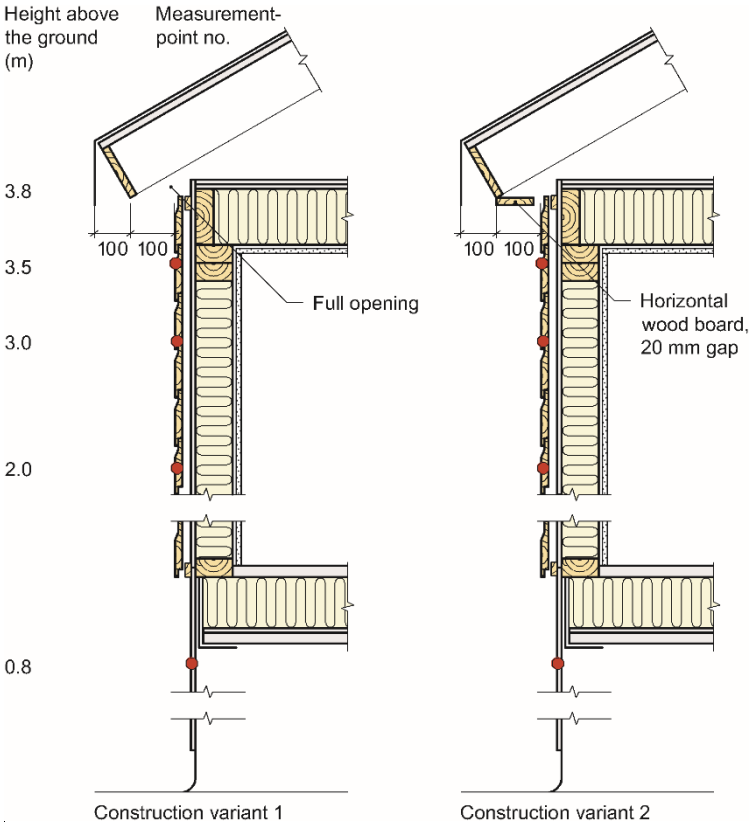

Fig. 5 Cross-section of the two wall sections studied in the field measurements. Red dots represent positions of the wind pressure measurements reported in the study.

Table 1: Accuracy and measuring range of applied sensors

Sensor	Manufacturer	Type	Accuracy	Range
Pressure transmitter	Furness Control	FCO 40	±5 % of reading	0–+1000 Pa
Wind direction	Lambrecht	-	±2°	0–360 °
Wind speed	Lambrecht	-	±5°	0.3-60 m/s

2.2 Uncertainty assessment

The root-mean-square (RMS) method was used to derive the uncertainty propagation of the measured c_p-values (equation (5)).

$$\frac{\Delta^P c_{px}}{c_{px}} = \sqrt{\left[\frac{\Delta^P P_\Delta}{P_\Delta}\right]^2 + \left[\frac{\Delta^P P_d}{P_d}\right]^2} \qquad (5)$$

Where $\frac{\Delta^P P_\Delta}{P_\Delta}$ is the uncertainty of P_Δ, which is defined as $P_\Delta = P_x - P_0$. $\frac{\Delta^P P_d}{P_d}$ is the uncertainty of P_d given by equation (2). No correlation between the terms of the balance equation was found.

Input data for this investigation was recorded wind speed measurements at 6m height above ground level of a wind mast and wind speed measurements at 10m above ground level. Identical anemometers to measure wind speed were used for the roof and wind mast measurements. NS-EN 1991-1-4:2005+NA:2009 (section 4.3 and NA) was used to calculate the wind speed at a height of 10m from the data in the wind mast at 6m height.

3. Results

The c_p of construction variant 2 at different positions on the cladding of the building is given in Figure 6. The pressure measurements are positioned on the exterior surface of the cladding. Four different wind approach angles are included in Figure 6: 0, 45, 90 and 180° ± 10°. An angle of 0° means that the wind approach angle is perpendicular to the wall.

The measured c_p at the surface of the cladding in different positions along the eaves of the house varies with different wind approach angles and position along the wall.

Figure 7 gives the mean (time averaged) c_p for construction variant 1 at 3.5 metre height given different wind approach angles.

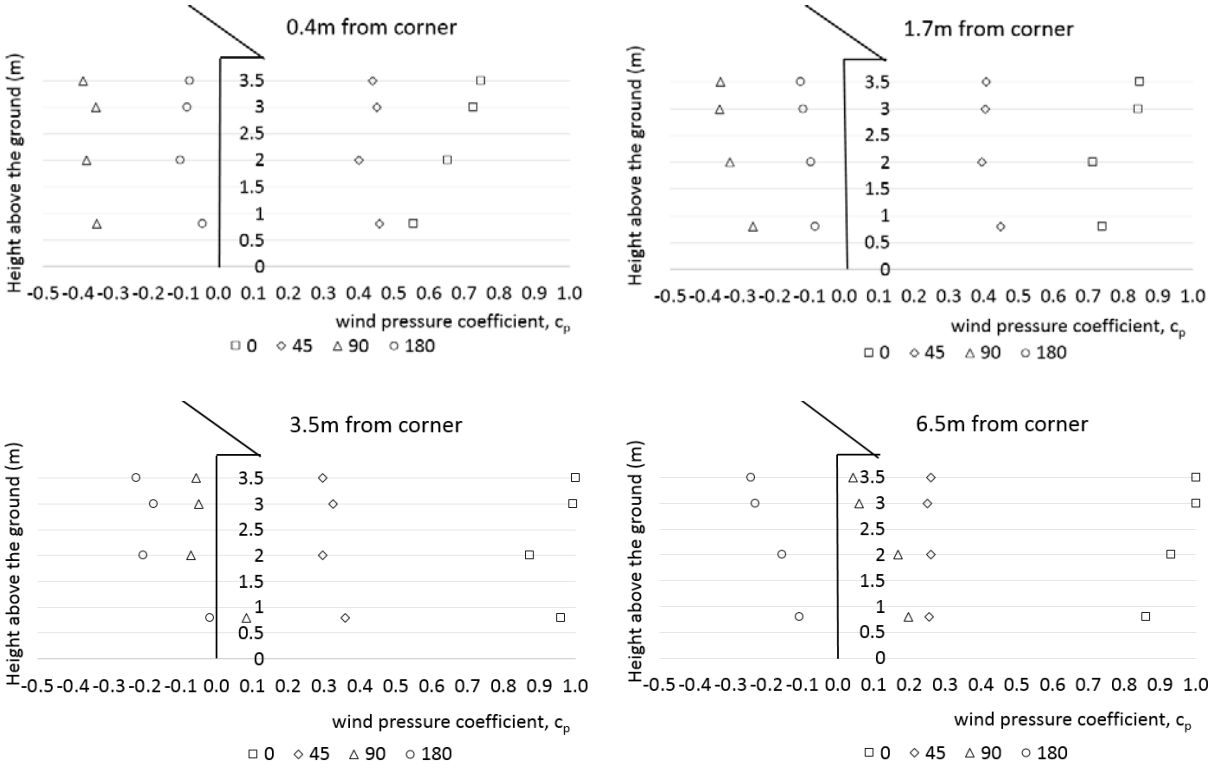

Fig. 6 Measured wind pressure coefficient, c_p, at positions 0.4m, 1.7m, 3.5m and 6.5 m from the corner; see black circle in Figure 7. Results for the wind approach angles 0°, 45°, 90° and 180°. All results are for construction variant 2.

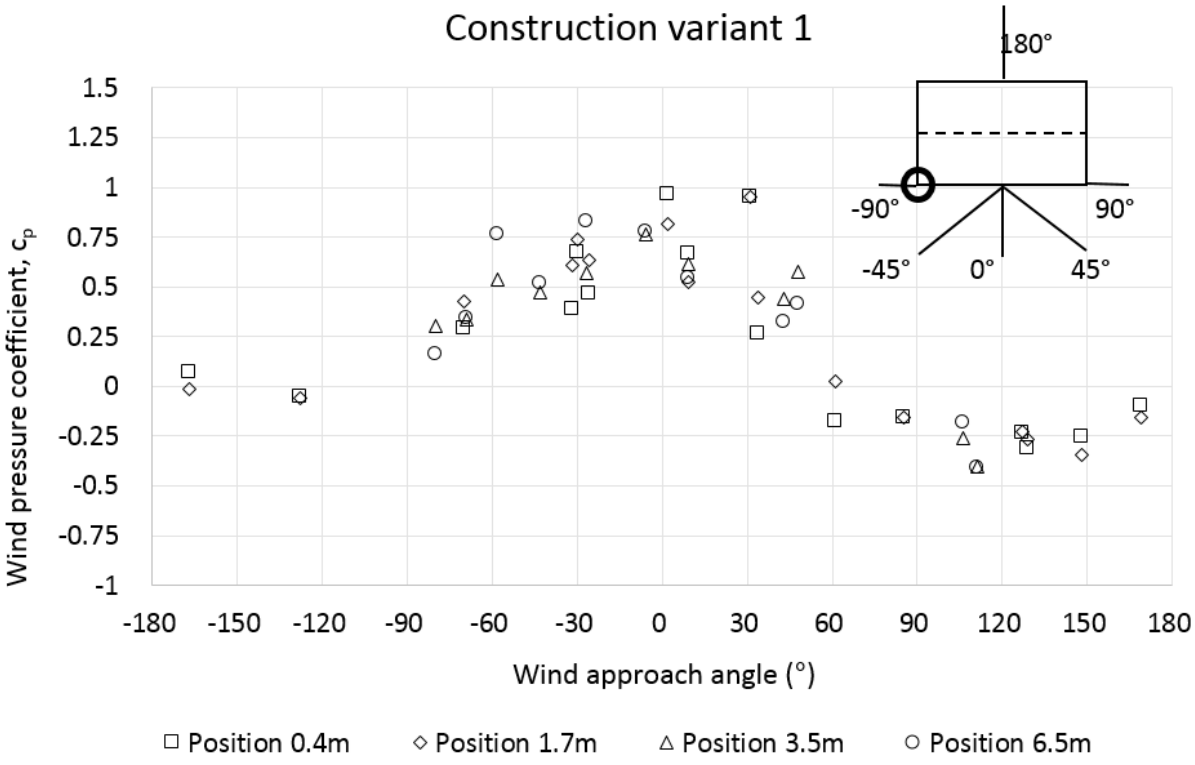

Fig. 7 Measured wind pressure coefficients, c_p, at four locations on the long wall, 3.5m above the ground and different wind approach angles (0° = perpendicular to the wall) for construction variant 1. Black circle in the upper-right corner of the diagram shows the corner from which the positions are measured.

Tokyo Polytechnic University has released a large and very detailed database on wind tunnel tests on low-rise buildings (Tokyo Polytechnic University, 2007). Parts of the database are published in Muehliesen and Patrizi (2013). According to the current study the values D/H=2.0 and D/B=1.0 matches best with the geometry of the test house. The exact values for the test house are D/H=8.0/3.8=2.11 and D/B=8.0/5.0=1.6. D,H and B are defined in Figure 4.

In Figure 8 c_p -values from Muehliesen and Patrizi (2013) are plotted together with mean (time averaged) results from construction variant 2 at a height of 3.5m given different wind approach angles.

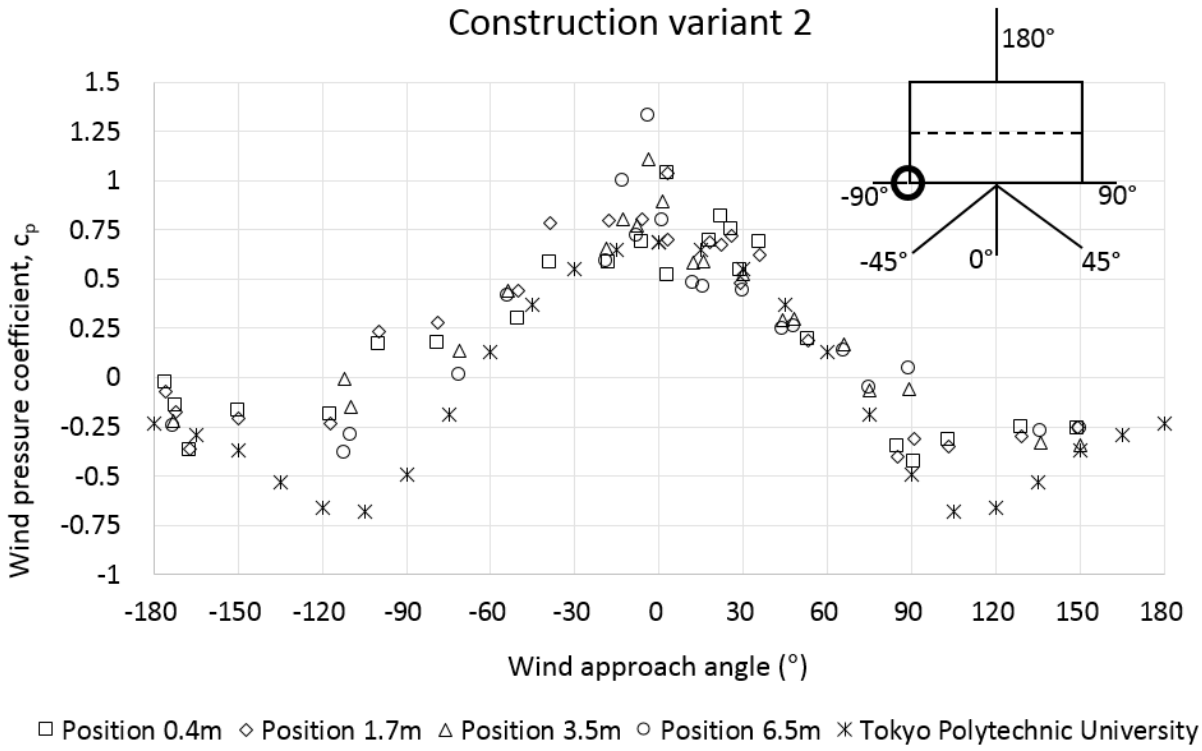

Fig. 8 Measured wind pressure coefficients, c_p, at four locations on the long wall 3.5m above the ground and different wind approach angles (0° = perpendicular to the wall) for construction variant 2. Black circle in the upper-right corner of the diagram shows the corner from which the positions are measured.

The c_p on the building facade according to NS-EN 1991-1-4:2005 together with the distribution of the measured c_p as a function of the wind approach angle is given in Figure 9.

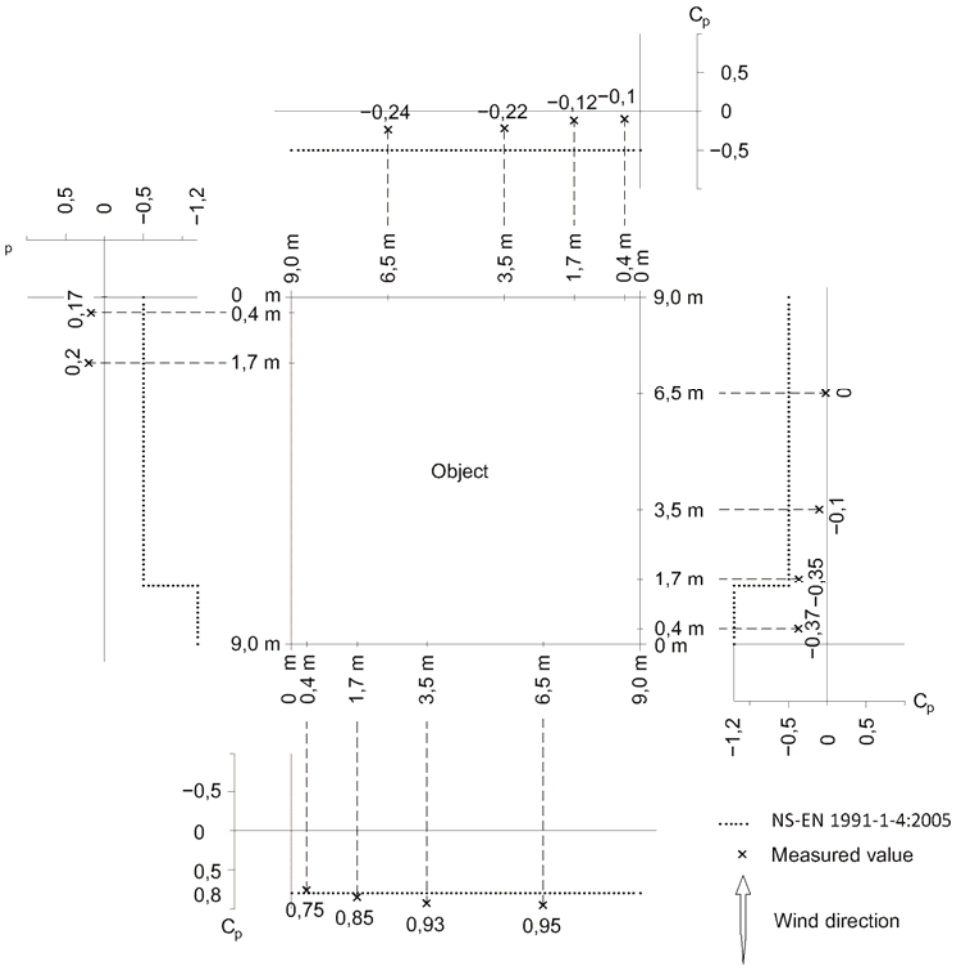

Fig. 9 Comparisons of c_p obtained by the measurements at 3.5m height above ground level, near the roof eave from this study and standard design values from NS-EN 1991-1-4:2005.

In general, the wind pressure difference between the inlet and the outlet of the air gap is the driving force for the wind-driven air change rate of the air gap beneath the roofing (see Figure 1). For engineering evaluation purposes, a simple method to calculate the air flow in the air gap and a procedure to estimate the pressure difference is needed. An average wind pressure factor difference, $\overline{\Delta c_p}$, has been derived based on the wind pressure measurements near the roof eaves at a height of 3.5m above ground level. The calculation was performed by averaging the measurements of c_p at wind approach angles of 0, 30, 45, 60, 90, 120, 135, 150, 180 ± 10° at the different positions of the wall (0.4m, 1.7m, 3.5m from the corner). $\overline{\Delta c_p}$ was calculated using equation (4). Looking at Figure 9 this means that for example, that:

Δc_p (0)= c_p (0)0.4m-c_p(180)0.4m =0.75- (-0.1)=0.85

The resulting average value derived from all approach angles and positions was $\overline{\Delta c_p}$ =0.7.

The calculated wind speed at 10m in the wind mast was compared to the measured wind speed at 10m, 4m above the ridge and positioned in the centre of the test house. A ratio of the two wind speeds has been calculated by dividing the measured value by the calculated value. The results have been sorted into two categories (see Figure 10). The global wind angle in the measurement period was 0-41°. Figure 10 contains all available measurement data.

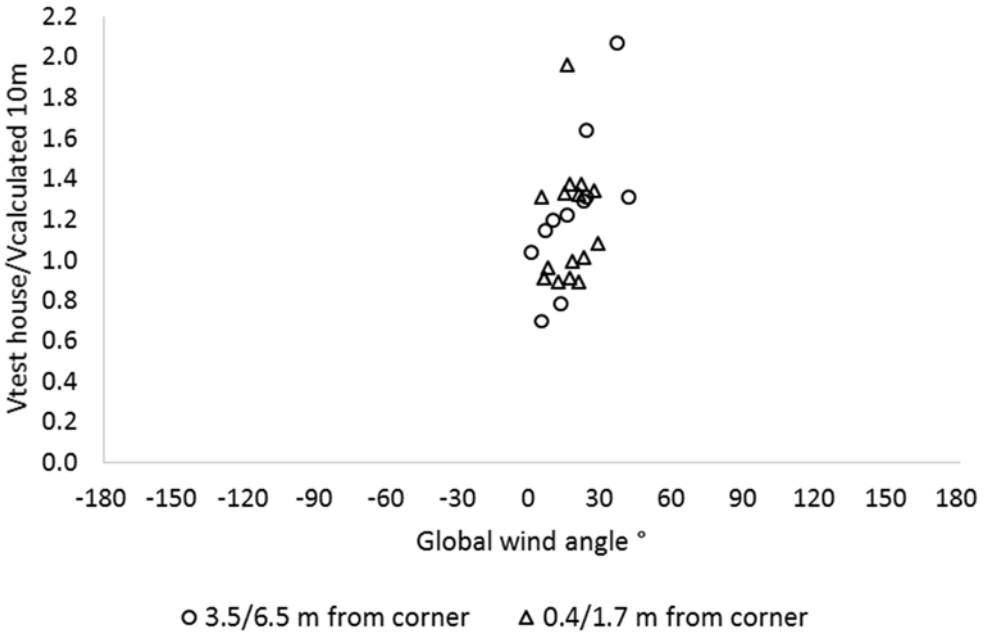

Fig.10 Ratio of the wind speed measured on the test house compared to calculated wind speed in a mast at 10m above ground level as a function of the global wind approach angle. The wind mast was positioned 40m away from the test house (as per Figure 3).

4. Discussion

4.1 Wind pressure coefficient

The largest positive c_p values were measured at the top of the middle section of the wall, given a wind approach angle perpendicular to the wall. The largest negative values were measured at the top of the wall, near the corner, at the wind approach angle of 90°, i.e. parallel to the wall. Both the distribution of the c_p on the building facade and the values of the c_p are in line with the investigations performed by Tominaga et al. (2015), Yang et al. (2008), Richardson and Blackmore (1995), Kanda and Maruta (1993) and Hoxey (1991). However, compared to the current study none of the previous field investigations includes the same amount of wind approach angles and measuring points on a building facade.

In general, a similar pressure distribution is found for c_p as a function of the wind approach angle for the measured c_p -values and the database from Tokyo shown in Figure 8 (Tokyo Polytechnic University, 2007). Both investigations show largest c_p-values for the 0° wind approach angle. The largest negative c_p-value was found for the wind approach angle of ±120°. For the wind approach angle of ±90-150° the calculated c_p values from the measurements differ somewhat compared to the Tokyo database values. One possible explanation is differences in the shape of the test building compared to the one used for the Tokyo database. The D/H value of the test building was 2.11 while the corresponding value from the database was 2.0. The D/B of the test house was 1.6 compared to 1.0 from the database. The values from the database show that both the D/H-values and the D/B-values have a significant impact on the c_p, especially for the wind approach angles between ±60 and 180°. This is also the interval with the largest deviation between the measurements and the values from the Tokyo database.

The Tokyo database results are from model measurements performed in a wind tunnel. In a wind tunnel, it is of course easier to control both wind speed and direction compared to field measurements where both the wind speed and direction fluctuate. This might explain part of the difference between the model measurements and the field measurements. However, field measurements reproduce natural conditions to a greater extent than laboratory measurements.

At a wind approach angle of 0°, the measured and NS-EN 1991-1-4:2005 values correspond. However, for the additional approach angles the c_p is overestimated by the standard. Values in NS-EN 1991-1-4:2005 are typically used to obtain design values for wind loads on building components. Therefore, it can be anticipated that the values from the standard gives conservative values for the c_p.

4.2 Design variants

There are fewer measuring values for construction variant 1 compared to variant 2 because the measurements were taken during different periods as the roof overhang was redesigned between the two measurements. The c_p-values of construction variant 1 and 2 are rather similar, showing the largest positive c_p for the wind approach angle of 0°, and the largest negative c_p at ±120-150°. In particular, there are small differences in c_p for the wind approach angles 0-180°. However, the c_p for the wind approach angles -0- to -180° shows differing data points, especially for wind approach angles of -90 to -180°. Missing measurement data for these wind approach angles for variant 1 makes it difficult to draw conclusions. The results indicate that the design of the eaves affects the wind pressure coefficient at the upper part of the facade to a small extent.

4.3 Test set up

In order to evaluate the driving forces of the vented air cavity the wind pressure coefficients at the air cavity openings beneath the roofing are highly relevant. In this specific case the horizontal roof overhang is 0.2m and the pressure measuring points are positioned 0.25m below the horizontal part of the roof overhang. The position was chosen so as to produce as general values as possible. From a practical perspective, the dimension of the roof overhang is project specific, as is the position of the air inlets in the horizontal part of the roof overhang. A trend in Nordic architecture is for slim eaves resulting in the gutter being nearly at the surface of the cladding. Figure 6 shows how the c_p varies with the height above the ground and the position along the wall. The roof overhang is identical for all the measurements. According to NS-EN 1991-1-4:2005 the c_p on the wall beneath the roof overhang is equal to the c_p at the top of the wall. Additionally, Blom (1990) states that the difference in the c_p of the upper part of the wall and beneath the roof overhang is rather small. Given no roof overhang, Figure 2 indicates that the roof angle affects the c_p at the upper part of the wall to a small extent.

Previously, Caracoglia and Jones (2009) used a sampling period of 300 seconds, and Wells and Hoxey (1980) used a sampling period of 240 seconds. However, the purpose of the current study was to produce wind pressure coefficients at specific wind approach angles. By increasing the sampling period, the variance in the wind approach angle will also increase. This was also stated by Wells and Hoxey (1980) who developed a method to take this into account. However, both Caracoglia and Jones (2009) and Wells and Hoxey (1980) performed measurements on houses that could not be rotated. The current measurements were performed using a rotatable test house in order to achieve specific wind approach angles and therefore shorter measuring periods were chosen. The ten second measuring period was chosen to enable as many measurements as possible to be taken and to reduce the variations in wind approach angle.

The wind measurement location was chosen in order to get standardised static and dynamic pressures at a height of 10m. The wind pressure measurements were conducted by direct measurement of the pressure difference of the static pressure at 10m to the static pressure at the surface of the cladding. As there was only 4m between the ridge and the position of the static and the dynamic wind pressure measurement device the measurements can probably not be considered a free-stream wind field. However, direct measurements of pressure difference require a location close to or on the test house in order to ensure a close distance between the measuring points on the facade and the wind measurement. Therefore, the test set up minimises the time lag between the wind gust hitting the facade and the wind reference. This was also why an identical length of all plastic tubes for the different measuring positions was used.

The distance between the wind measuring device at the test house and in the wind mast was 40m. The calculated ratio of the measured wind speed at the test house and at the wind mast in Figure 10 gives the instant wind speed difference. The global wind approach angle has a direct influence on this ratio. For some global wind approach angles there will be a significant time lag between the wind front hitting the test house and the wind mast. A global wind approach angle perpendicular to the line through the test house and the wind mast will lower the latter time lag as much as possible. Hence, a global wind approach angle of south-southwest (~20°) gives the smallest time lag. By analysing the data for this wind approach angle a ratio of 1.27 was calculated. That implies that on average the wind speed 4m above the ridge of the test house is 27% higher than the calculated wind speed at a height of 10m in the wind mast. In turn, this gives a reduced value of c_p according to equation (1). The difference in static pressure at the two locations was, however, not measured and therefore evaluation of the static pressure difference at the two locations is lacking.

According to NS-EN 1991-1-4:2005 and the previous results of Tominanga et al. (2015) and Ahmad and Kumar (2002) the results from the current study can be applicable for one to two-storey houses with pitched roof and different roof angles. The measurements from Ahmad and Kumar (2002) show increasing c_p -values with increasing building heights.

Uncertainty of wind pressure measurements

It has not been possible to evaluate the error in measured c_p. The following points indicate the possible sources and levels of error.

1) Each of the measured local loss coefficients consist of 20 measurements. The calculation of the wind pressure coefficient is based on the ratio of the pressure difference of the facade and the static pressure at a height of 10m and the dynamic pressure at a height of 10m. By assuming ± 5 % of reading accuracy the uncertainty of the measurements can be calculated to 7%.

2) The test house affects the dynamic wind pressure measurements performed in 4m height above the ridge. On average the wind speed 4m above the ridge of the test house is 27% higher than the calculated wind speed at a height of 10m in the wind mast. In turn, this gives a reduced value of c_p according to equation (1). However, the difference in static pressure at the two locations has not been measured.

4.4 Practical use

As previously stated Δc_p is essential when calculating the wind-driven ventilation of the air cavity below the roofing. When using Δc_p for ventilation purposes the Δc_p is calculated by equation (4) assuming that the roofing is ventilated by air flowing directly through the roof structure. However, in a real situation the air change rate of the air cavity beneath the roofing is strongly dynamic and affected by several parameters among them the design and position of the air cavity openings as well as the design of the air cavity beneath the roofing. As Cóstala et al. (2009) mentioned, the typical wind approach angle is also dependent on the location and orientation of the specific house. Calculations of ventilation of roofing in practice require simplifications regarding both wind approach angle and typical wind velocity.

In practical calculations of the ventilation of the air cavity beneath the roofing it is necessary to assume a conservative wind speed and -approach angle at the location of the roof structure. In such cases an average value of Δc_p is valuable for estimating the ventilation of the roof cavity.

In this work a $\overline{\Delta c_p}$ of 0.7 was derived by assuming that the roofing is ventilated by air flowing directly through the roof structure (see Figure 1). By studying the results from Tominaga et al. (2015),

Richardson and Surry (1991) and Zisis and Stathopoulos (2012) the authors found a Δc_p of 0.5-1.4. The results from the current study are in line with the results from these previous studies. Results from Zisis and Stathopoulos (2012) show a larger Δc_p given a more urban terrain. The impact from sheltering is not a part of this study, but might influence the c_p and therefore needs to be further investigated.

In practice, roofing materials might often have openings in the ridge of the roofing. Openings in the air cavity positioned at different heights introduces natural convection as a driving force of air change in the air cavity. The results from the study only apply to ventilation from eaves to eaves, as shown in Figure 1. Wind pressure coefficients on different pitched roofs were measured by Ahmad and Kumar (2002) and Tominaga et al. (2015), see Figure 2. As the results from these studies show, there is a negative wind pressure coefficient at the ridge depending on the height above ground and pitch of the roof. Given openings in the ridge, in practice the roofing will be ventilated both through the ventilation opening in the ridge and from eaves to eaves, as shown in Figure 1. However, for a winter situation with snow on the roof the situation will be as shown in Figure 1. The distribution between the air cavity ventilation through the eaves-ridge and eaves-eaves of the roof has not been part of the current study, but also needs to be further investigated.

5. Conclusion

The paper describes detailed full-scale measurements of wind pressure coefficients on a rotatable test house. The large-scale test measurements show that the wind pressure coefficient along the eaves of the house vary with different wind approach angles. Furthermore, the measurements show increasing c_p at the upper, middle part of the wall. Both the distribution of the c_p on the building facade and the values of the c_p are in line with previous field and laboratory investigations.

A $\overline{\Delta c_p}$ of 0.7, needed for engineering evaluations, was calculated by assuming that the roofing is ventilated by air flowing directly through the roof structure. The results from the study are applicable for one to two-storey buildings with pitched roof and different roof angles.

Acknowledgements

The authors gratefully acknowledge the financial support of the Research Council of Norway and several partners through the Centre of Research-based Innovation "Klima 2050" (www.klima2050.no). A special thanks to CAD operator Bjørnar Nørstebø and Remy Eik. The authors also gratefully acknowledge the anonymous Journal of Wind Engineering & Industrial Aerodynamics referees for valuable comments on the text.

References

Ahmad S, Kumar K. (2002) Effect of geometry on wind pressures on low-rise hip roof buildings. *Journal of Wind Engineering & Industrial Aerodynamics* 90: 755-779.

Bartko M, Molleti S, Baskaran A. (2016) In situ measurements of wind pressures on low slope membrane roofs. *Journal of Wind Engineering & Industrial Aerodynamics* 153: 78-91.

Blom P. (1990) Ventilasjon av isolerte skrå tak. (Ventilation of pitched wooden roofs)(In Norwegian) PhD thesis 1990:39. NTH. Norway

Bøhlerengen T. (2007) 525.101 Isolerte skrå tretak med lufting mellom vindsperre og undertak. (Pitched wooden roofs with ventilation between the wind barrier and the underlayer roofing)(In Norwegian) SINTEF Building Design Guides. SINTEF. Oslo

Bøhlerengen T. (2012) 525.102 Isolerte skrå tretak med kombinert undertak og vindsperre. (Pitched wooden roofs with combined underlayer roof and wind barrier)(In Norwegian) SINTEF Building Design Guides. SINTEF. Oslo

Caracoglia L, Jones NP. (2009) Analysis of full-scale wind and pressure measurements on a low-rise building. *Journal of Wind Engineering and Industrial Aerodynamics* 97: 157-173.

Cóstola D, Blocken B, Hensen JLM. (2009) Overview of pressure coefficient data in building energy simulation and airflow network programs. *Building and Environment* 44: 2027-2036.

Edvardsen K, Ramstad T. (2014) Trehus Håndbok 5. (Wood buildings handbook 5)(In Norwegian) SINTEF Building and Infrastructure. Oslo

Hoxey RP. (1991) Structural response of a portal framed building under wind load. *Journal of Wind Engineering & Industrial Aerodynamics* 38: 347-356.

Hoxey RP, Wells DA. (1974) Instrumentation for full-scale wind load measurement on glasshouses. *Journal of Agricultural Engineering Research* 19: 435-438.

Hoxey RP, Wells DA. (1977) Full-scale wind pressure measurements on a twin-span 12.2 × 12.2 m inflated roof greenhouse. *Journal of Wind Engineering and Industrial Aerodynamics* 2: 211-221.

Kanda M, Maruta E. (1993) Characteristics of fluctuating wind pressure on long low-rise buildings with gable roofs. *Journal of Wind Engineering and Industrial Aerodynamics* 50: 173-182.

Muehleisen RT, Patrizi S. (2013) A new parametric equation for the wind pressure coefficient for low-rise buildings. *Energy & Buildings* 57: 245-249.

NS-EN 1991-1-4:2005. Eurocode 1: Actions on structures Part 1-4: General actions Wind actions. Standard Norge.

Quan Y, Liang Y, Wang F, Gu M. (2011) Wind tunnel test study on the wind pressure coefficient of claddings of high-rise buildings. *Selected Publications from Chinese Universities* 5: 518-524.

Richardson GM, Blackmore PA. (1995) The Silsoe structures building: Comparison of 1 : 100 model-scale data with full-scale data. *Journal of Wind Engineering and Industrial Aerodynamics* 57: 191-201.

Richardson GM, Surry D. (1991) Comparisons of wind-tunnel and full-scale surface pressure measurements on low-rise pitched-roof buildings. *Journal of Wind Engineering and Industrial Aerodynamics* 38: 249-256.

Tokyo Polytechnic University. (2007) Aerodynamic Database of Low-Rise Buildings, http://www.wind.arch.t-kougei.ac.jp/info_center/windpressure/lowrise/mainpage.html (last accessed 16.11.2016)

Tominaga Y, Akabayashi S-I, Kitahara T, Arinami Y. (2015) Air flow around isolated gable-roof buildings with different roof pitches: Wind tunnel experiments and CFD simulations. *Building and Environment* 84: 204.

Uematsu Y, Isyumov N. (1999) Wind pressures acting on low-rise buildings. *Journal of Wind Engineering and Industrial Aerodynamics* 82: 1-25.

Uvsløkk S. (1996) The Importance of Wind Barriers for Insulated Timber Frame Constructions. *Journal of Building Physics* 20: 40-62.

Wells DA, Hoxey RP. (1980) Measurements of wind loads on full-scale glasshouses. *Journal of Wind Engineering and Industrial Aerodynamics* 6: 139-167.

Xu YL, Reardon GF. (1998) Variations of wind pressure on hip roofs with roof pitch. *Journal of Wind Engineering & Industrial Aerodynamics* 73: 267-284.

Yang W, Quan Y, Jin X, Tamura Y, Gu M. (2008) Influences of equilibrium atmosphere boundary layer and turbulence parameter on wind loads of low-rise buildings. *Journal of Wind Engineering and Industrial Aerodynamics* 96: 2080-2092.

Zisis I, Stathopoulos T. (2012) Wind load transfer mechanisms on a low wood building using full-scale load data. *Journal of Wind Engineering and Industrial Aerodynamics* 104-106: 65-75.